

Study on Facile Preparation of Composite Photocatalyst Based on Titanium Dioxide and Their Photocatalytic Hydrogen Evolution Performance

Xinxin Jiang, Masayoshi Fuji

Advanced Ceramics Research Center, Nagoya Institute of Technology
3-101-1 Honmachi, Tajimi, Gifu 507-0033, JAPAN

Abstract

As an important area in the field of advanced materials, TiO₂-based photocatalysts have always been researched hot pots. At present, most of the applications of TiO₂-based photocatalysts are still in the experimental stage. This research uses commercial TiO₂ as the main material and aims to simplify the synthesis method and reduce the experimental cost. This work uses the co-catalyst as the starting point to investigate a metal co-catalyst, sulfide co-catalyst, and phosphide co-catalyst. Cu, MoS_x and MoP are respectively used to construct a catalytic system to improve the photocatalytic hydrogen production ability of the material. Good loading methods are applied, such as in-situ photo-deposition, ultrasonic adsorption, etc., to optimize the synthesis steps, promote the transfer of electrons and holes between the different materials and improve the photocatalytic performance of the composite materials. The photocatalytic reaction mechanism was revealed by studying the morphology of the catalyst, the combination mode, the separation efficiency of the photogenerated carriers, and the photocatalytic hydrogen production activity under ultraviolet light. The results of this study provide technical support and a theoretical basis for the design and preparation of low-cost, simple and efficient photocatalytic systems.

Keywords: Titanium dioxide, molybdenum phosphide, molybdenum sulfide, cuprous oxide, photocatalysts, hydrogen.

1. Introduction

Photocatalytic technology is expected to play an important role in future energy expansion by solving the increasingly serious energy depletion and environmental deterioration. As an important field of advanced materials, TiO₂-based photocatalysts have always been studied as hot spots. Titanium dioxide itself has a photocatalytic activity in the ultraviolet region. However, it is still in the experimental stage. The easy recombination of high numbers of photogenerated electrons and holes reduces the number of active species that can cause redox reactions and impedes the TiO₂ photocatalytic performance. The co-catalyst composite photocatalysts are an effective way to solve this problem. Not only are some co-catalysts cheaper and easier to synthesize, but they also provide internal electron transfer channels in the composite to facilitate charge transfer in the photocatalyst and improve its ability to generate hydrogen. Ni, Cu and their oxides, some transition metal sulfides (such as MoS₂, WS₂, NiS and CuS, etc.) and transition metal phosphides (such as NiP, MoP, CoP, CuP, etc.) are used as non-precious metal hydrogen evolution promoters. and received widespread attention.

Cu₂O has a bandgap of 2.2eV and is a p-type semiconductor. Recent literature has shown that Cu₂O supported by TiO₂ can act as a cocatalyst for photocatalytic hydrogen production with performance comparable to Ag and Au^[1, 2]. In addition, part of the Cu⁺ particles is reduced to Cu (0) particles during the photocatalytic process, which can effectively improve the carrier transfer efficiency during the photocatalytic process^[3].

Molybdenum phosphide (MoP) has attracted extensive attention due to its platinum-like electronic structure, low synthesis cost, high catalytic activity, and acid and alkali resistance. According to density functional theory (DFT) calculations, the P atoms in transition metal phosphides (TMPs) play an important part in the hydrogen production process. Owing to its high electronegativity ($\chi = 2.1$), the P atom has a strong ability to extract electrons, so it can attract an electron from the metal atom when combined with a metal element^[4, 5]. Therefore, MoP is a potential cocatalyst to modify TiO₂ to enhance its photocatalytic activity.

Molybdenum sulfide has a special two-dimensional layered structure and is the most promising electronic promoter to replace the noble metal Pt. Numerous

studies have shown that TiO_2 modified with molybdenum disulfide (MoS_2) nanoparticles can significantly improve the performance of photocatalytic hydrogen production^[6, 7]. In addition, increasing the number of unsaturated S atomic active sites located at the material edge is an important strategy to enhance the photocatalytic hydrogen production performance of semiconductor materials^[8]. In general, the irregular arrangement of atoms in amorphous materials tends to form more atomic defect sites or unsaturated active sites than in crystalline materials. Therefore, the modification of semiconductor materials by synthesizing amorphous molybdenum sulfide (a-MoS_x) is a feasible way to improve photocatalytic performance.

Based on the above background, this study uses commercial titanium dioxide as the main material. Using cheap materials such as Cu, MoS_x , and MoP as cocatalysts, the synthesis method is simplified and the photocatalytic hydrogen production capacity of the materials is improved.

2. The design and preparation of $\text{TiO}_2/\text{Cu}_2\text{O}/\text{Cu}$ composite photocatalyst and its photocatalytic water splitting performance

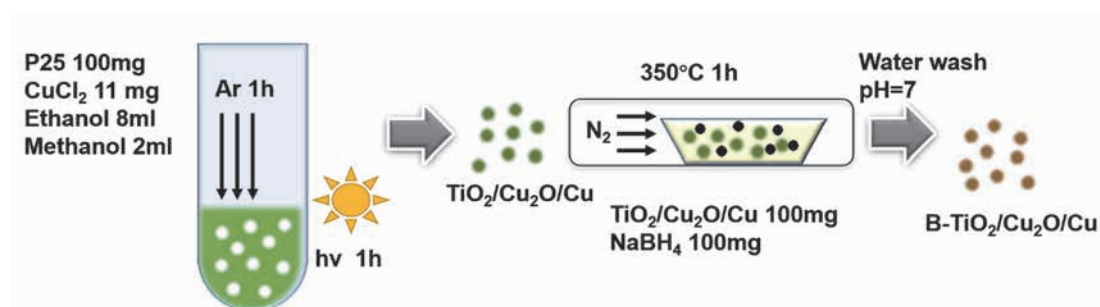
The $\text{B-TiO}_2/\text{Cu}_2\text{O}/\text{Cu}$ composite material was synthesized in two steps involving in-situ photodeposition and hydrogenation treatment. Briefly, commercial P25 (TiO_2) was dispensed in a test tube containing a solution of absolute ethanol and methanol. A specific amount of CuCl_2 was added and dissolved by stirring. Argon gas was used as a purge gas for half an hour, then irradiated with ultraviolet light for one hour to reduce the Cu particles on the surface of the TiO_2 to obtain the $\text{TiO}_2/\text{Cu}_2\text{O}/\text{Cu}$ powder. The $\text{TiO}_2/\text{Cu}_2\text{O}/\text{Cu}$ powder was then mixed with NaBH_4 powder and heated at a specific temperature, and the hydrogenation reaction occurred. The hydrogenated $\text{TiO}_2/\text{Cu}_2\text{O}/\text{Cu}$ powder was then obtained. A schematic diagram of the whole process was shown in Scheme 1. The $\text{TiO}_2/\text{Cu}_2\text{O}$ catalysts with

different annealing temperatures of 300 °C, 350 °C, and 400 °C, are called TC6-300, TC6-350, and TC6-400, respectively. The $\text{TiO}_2/\text{Cu}_2\text{O}$ catalysts with different content Cu, called TC2, TC4, TC6, TC8 and TC10, respectively (The nominal mass fraction of Cu relative to TiO_2 was 6 wt%, and the resulting sample was labelled TC6.). hydrogenated Cu_2O and TiO_2 powder, called H- $\text{Cu}_2\text{O}/\text{Cu}$ and B- TiO_2 .

Fig. 1 shows the X-ray diffraction measurements of each sample. The XRD results indicated that Cu_2O and Cu are in situ loaded on the surface of the TiO_2 .

Figure 2 shows TEM images of the B- $\text{TiO}_2/\text{Cu}_2\text{O}/\text{Cu}$ (TC6-350) sample which can more clearly be used to observe the distribution of copper particles on the TiO_2 surface. The TEM surface morphology shows the presence of $\text{Cu}_2\text{O}/\text{Cu}$ particles on the TiO_2 surface as small islands or surface deposits.

The photocatalytic activity of the prepared samples was evaluated by a hydrogen evolution test. As shown in Figure 3, the photocatalytic activity of pure TiO_2 and B- TiO_2 for water splitting under ultraviolet irradiation is very poor. Comparing the TC6 sample with the BTC6 sample, it can be seen that due to the reduction of the specific surface area of the TiO_2 after the hydrogenation treatment, the copper precursor adsorbed on the surface of the titanium dioxide decreases during the photodeposition process (Table 1). As a result, the actual copper content of the BTC6 sample is much lower than that of the TC6 sample, which ultimately leads to a decrease in the hydrogen evolution performance. When $\text{Cu}_2\text{O}/\text{Cu}$ particles are deposited on the surface of TiO_2 , the photocatalytic hydrogen release capacity of $\text{TiO}_2/\text{Cu}_2\text{O}/\text{Cu}$ is enhanced. When the copper loading reaches 6%, the TC6 sample reaches the maximum hydrogen evolution efficiency. After the hydrogenation treatment, the photocatalytic hydrogen release ability of the B- $\text{TiO}_2/\text{Cu}_2\text{O}/\text{Cu}$ sample is further enhanced. The maximum release of TC6-350 under ultraviolet light is about $8.5\text{mmol h}^{-1}\text{g}^{-1}$, which is 40 times that of the



Scheme 1 Schematic illustration for the synthesis route of the B- $\text{TiO}_2/\text{Cu}_2\text{O}$ nanoparticles (TC6-350).

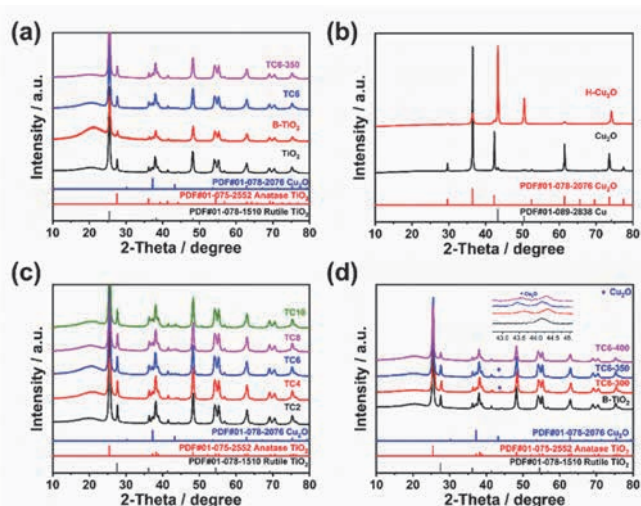


Fig. 1 XRD patterns of the as-prepared samples: (a) TiO_2 , B- TiO_2 , TC6 and TC6-350, (b) $\text{Cu}_2\text{O}/\text{Cu}$ and Hydrogenated $\text{Cu}_2\text{O}/\text{Cu}$, (c) $\text{TiO}_2/\text{Cu}_2\text{O}/\text{Cu}$ with different copper loadings, (d) TC6 samples formed at different hydrogenation temperatures.

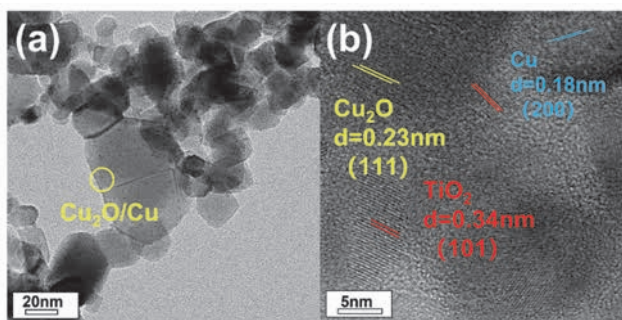


Fig. 2 TEM and HR-TEM images of the B- $\text{TiO}_2/\text{Cu}_2\text{O}/\text{Cu}$ (TC6-350) sample

hydrogen evolution rate of pure TiO_2 . With the increase in the hydrogenation temperature, the photocatalytic activity of the B- $\text{TiO}_2/\text{Cu}_2\text{O}/\text{Cu}$ samples first increased, then decreased^[9]. The decrease in performance with the increasing annealing temperature can be attributed to two aspects. (1) The specific surface area is reduced. The results show that the lower specific surface area of

the sample has a greater impact on its catalytic performance^[10]. (2) The concentration of bulk defects increases. Titanium dioxide has two kinds of defects, namely bulk defects and surface defects^[11]. The surface defects can trap carriers and transfer them to surface-adsorbed materials to promote the separation of photogenerated electrons and holes. The bulk defects will trap carriers and recombine them. As the annealing temperature increases, the concentration of the bulk defects increases, thereby reducing the catalytic performance of the sample. This is consistent with the PL result. This phenomenon has also been reported in a previous publication^[12].

Scheme 2 illustrates the mechanism of the photocatalyst. When Cu_2O is loaded on the surface of B- TiO_2 , the B- $\text{TiO}_2/\text{Cu}_2\text{O}$ hybrid exhibits an n-n semiconductor system. Due to the relative position of the energy band potential, the photogenerated electrons are transferred from the conduction band of Cu_2O (-0.41eV) to the conduction band of B- TiO_2 (-0.32eV). In addition, the Fermi energy level of Cu is lower than that of the n-type Cu_2O and B- TiO_2 . The electrons on the CB of TiO_2 can further migrate to Cu until the system reaches equilibrium, and the photogenerated electrons reduce H^+ to H_2 on the surface of the copper particles. At the same time, the photo-generated hole on the valence band of the B- TiO_2 is inserted into the valence band of Cu_2O , and the methanol adsorbed on the surface is oxidized, thereby inhibiting the recombination of the charge carriers. Due to the synergistic effect of the B- $\text{TiO}_2/\text{Cu}_2\text{O}$ heterojunction and metallic copper particles, the copper-loaded black TiO_2 helps to expand the light absorption range, improve the separation efficiency of the carriers, and improve the photocatalytic hydrogen evolution ability. Therefore, B- $\text{TiO}_2/\text{Cu}_2\text{O}/\text{Cu}$ is an attractive photocatalyst under ultraviolet radiation.

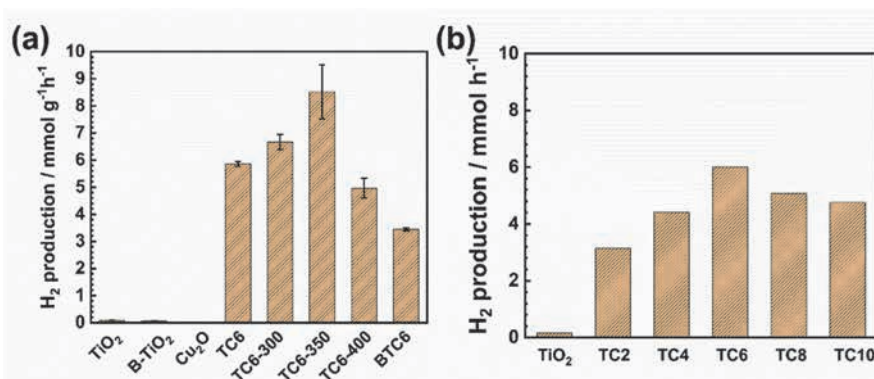
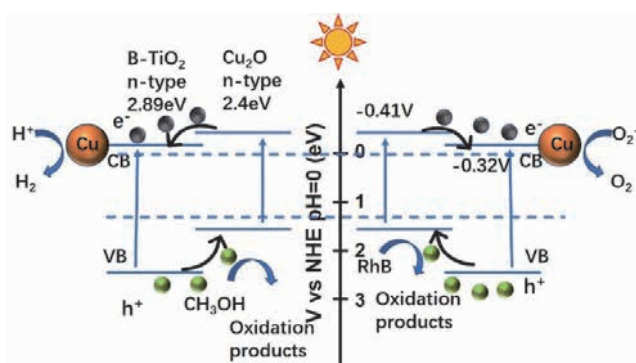


Fig. 3 Photocatalytic activity tests for H_2 evolution by the as-prepared samples under UV light

Table 1 Physical characteristics of the B-TiO₂/Cu₂O/Cu catalysts.

Catalyst	Specific surface area (m ² g ⁻¹)	pore volume cm ³ g ⁻¹
TiO ₂	50.7	0.401
B-TiO ₂	43.2	0.241
Cu ₂ O/Cu	5.64	0.04
BTC6	36.8	0.241
TC6	46.0	0.323
TC6-300	46.3	0.317
TC6-350	44.9	0.282
TC6-400	37.0	0.251

**Scheme 2** Scheme of the photocatalytic mechanism of the B-TiO₂/Cu₂O/Cu photocatalysts for the evolution of H₂ and degradation of the RhB.

3. The design and preparation of TiO₂/MoP composite photocatalyst and its photocatalytic performance for water splitting

In Chapter 2, the coordination effect of the copper cocatalyst and hydrogenation of TiO₂ successfully improved the hydrogen evolution performance of the catalyst. However, the preparation of the catalyst involves multiple synthesis steps, the experimental control is relatively complicated, and the preparation is relatively complicated. Since metallic copper particles are extremely easy to oxidize in the air and water, it is difficult to control the ratio of Cu¹⁺ and Cu (0) particles. This is not conducive to further optimising the catalytic performance.

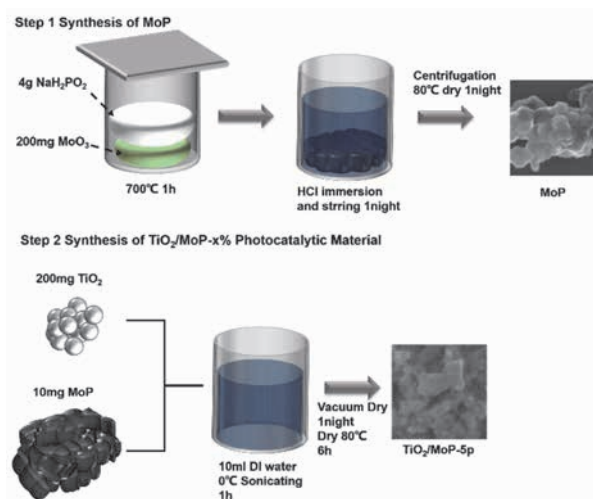
As far as we know, there are few reports about the modification of TiO₂ by MoP and its application to photocatalytic water splitting. During the photocatalytic preparation process, high-temperature calcination often causes changes in the catalyst, such as a decrease in the specific surface area and lack of active sites, resulting in a decreased photocatalytic performance. In this chapter, sodium hydrogen hypophosphite was used to

phosphorylate MoO₃ powder to prepare the MoP powder, which was combined with commercially-available TiO₂ using a simple ultrasonic dispersion method. The subsequent annealing steps are reduced, manufacturing costs are reduced, and the photocatalytic hydrogen generation performance is improved. A schematic diagram of the entire process is shown in Scheme 3.

The phase structure of the TiO₂/MoP photocatalyst can be characterized by an XRD pattern, as shown in Figure 4. Figure 4 shows the characteristic peaks of TiO₂ and MoP, indicating that the TiO₂/MoP composite was successfully synthesized.

Figure 5 shows a TEM image of the TiO₂/MoP-5p sample. The MoP particles are rougher than the TiO₂ particles and form uniform agglomerates with them, thus providing a good interface contact, exposing more surfaces/boundaries and increasing the active sites.

In Figure 6, we analyzed the hydrogen production efficiency of the TiO₂, MoP and TiO₂/MoP samples. The

**Scheme 3** Schematic illustration showing the synthesis route of the TiO₂/MoP nanoparticles.

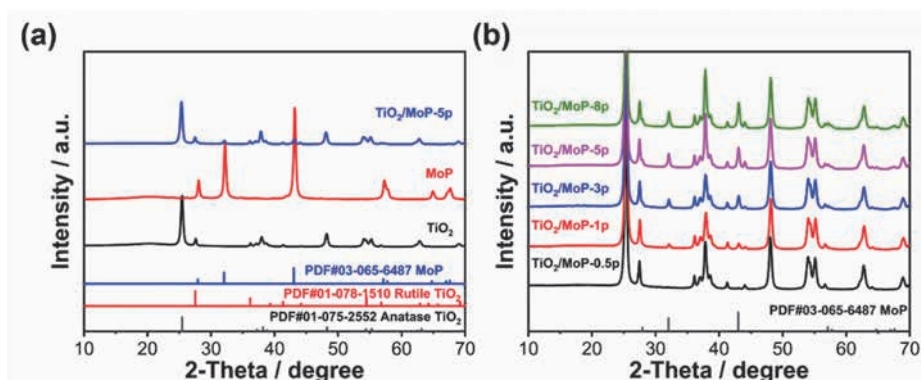


Fig. 4 (a,b) X-ray diffraction profile results of as-prepared samples

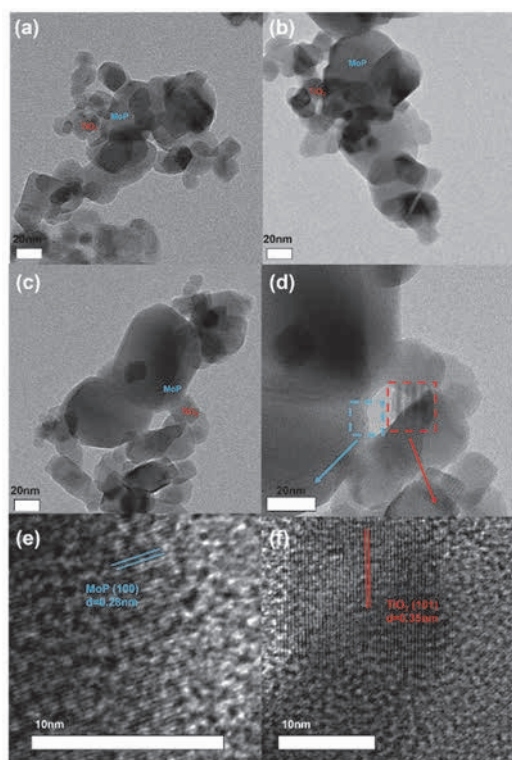


Fig. 5 TEM images of $\text{TiO}_2/\text{MoP-5p}$: (a), (b), (c), (d) and corresponding magnification of HRTEM image (e), (f).

pure TiO_2 photocatalyst has almost no photocatalytic activity. This is mainly due to the lack of high-efficiency electron promoters and the high electron-hole recombination rate^[13]. The pure MoP photocatalysts also have no photocatalytic activity, which is due to the metallic properties of MoP^[14]. When the TiO_2 photocatalyst was combined with MoP, the photocatalytic activity of all the TiO_2/MoP samples was significantly improved. With the increase in the MoP loading, the hydrogen evolution performance of TiO_2/MoP gradually improved. The hydrogen evolution rate of $\text{TiO}_2/\text{MoP-5p}$ is the highest, reaching $4.3\text{mmol g}^{-1}\text{h}^{-1}$. Compared to the TiO_2 photocatalyst, the photocatalytic hydrogen production performance of the TiO_2/MoP photocatalyst is improved 18-fold. To determine the stability of the TiO_2/MoP sample, four repeated experiments were carried out (Figure 6(b)). Obviously, the $\text{TiO}_2/\text{MoP-5p}$ sample was able to maintain a stable and effective hydrogen production rate during the repeated experiments. After the five repeated experiments, the hydrogen evolution rate remained at 64%. After four cycles of experiments, the hydrogen evolution performance of the sample rapidly dropped. This is due to the prolonged hydrogen evolution reaction and photo corrosion of the MoP co-catalyst.

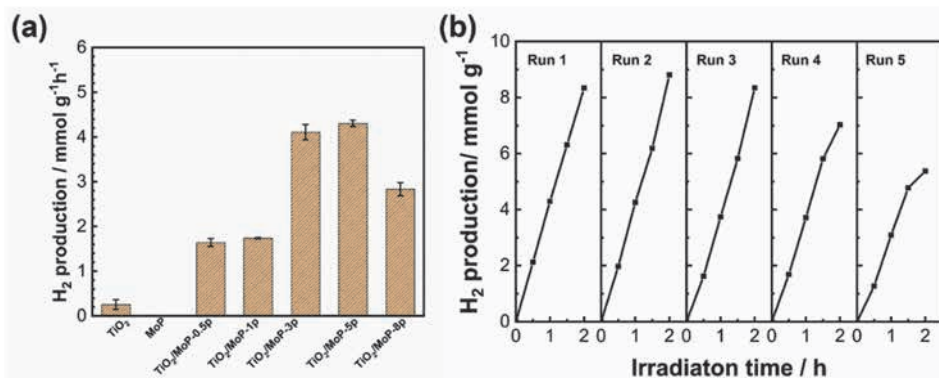
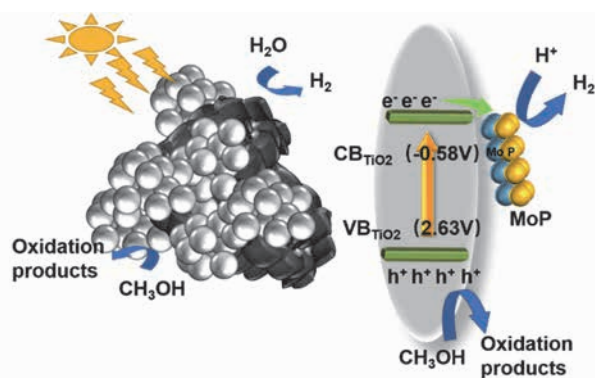


Fig. 6 (a) Photocatalytic activity tests for H_2 evolution by the as-prepared samples under UV light. (b) Photocatalytic stability of the $\text{TiO}_2/\text{MoP-5p}$ photocatalyst.

A possible mechanism is proposed to illustrate the improvement in the hydrogen production performance of the TiO_2/MoP catalyst, as shown in Scheme 4. When MoP is loaded on the surface of TiO_2 , the TiO_2/MoP hybrid exhibits a typical metal-semiconductor system. Under ultraviolet radiation, titanium dioxide can be quickly activated to generate photo-generated electrons and holes. Because the work function of the MoP (5.61 eV) is higher than that of TiO_2 (4.21 eV), electrons in the conduction band of the TiO_2 can be quickly transferred to the surface of the MoP particles instead of returning to the defect energy level or reducing the recombination of the VB and holes. Due to the better hydrogen affinity of MoP, H^+ is quickly captured and reduced to H_2 . At the same time, due to the high hole trapping ability of methanol, the holes can quickly oxidize the methanol on the TiO_2 surface. Due to the low impedance between the TiO_2 and MoP and the high-quality metal-semiconductor system, the developed TiO_2/MoP hybrid can effectively separate photo-generated electrons and holes and move them to the surface of the MoP and TiO_2 particles, respectively. This is the reason for the highly-enhanced photocatalytic hydrogen production activity.



Scheme 4 Schematic diagrams illustrating the possible photocatalytic mechanism of the TiO_2/MoP photocatalyst.

4. The design and preparation of $\text{TiO}_2/\text{MoS}_x$ composite photocatalyst and its photocatalytic performance for water splitting

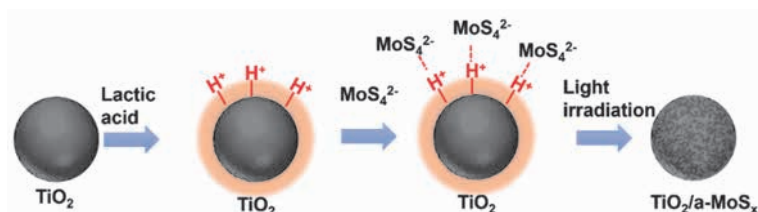
In the previous chapter, using MoP as a co-catalyst, a catalytic system with simple synthesis steps and a better hydrogen evolution performance was introduced. However, due to the limitation of the MoP preparation process, there are fewer active sites on the MoP body, which restricts the further improvement of its catalytic performance. How to use a simple method to prepare a cocatalyst with abundant active sites to construct a

catalytic system with high catalytic performance has become the research focus of this chapter. In this study, we synthesized an amorphous molybdenum sulfide electron co-catalyst-modified TiO_2 ($\text{TiO}_2/\text{a-MoS}_x$) photocatalytic material by the in-situ adsorption-photodeposition conversion method to improve the photocatalytic hydrogen production performance. Briefly, P25 was mixed with the ammonium tetrathiomolybdate, then by light irradiation, the ammonium tetrathiomolybdate was reduced to molybdenum sulfide and adsorbed on the surface of the TiO_2 . A schematic diagram of the whole process is shown in Scheme 5. When the Mo content is 0.1, 0.5, 1, 3, 5, and 8 wt%, the obtained $\text{TiO}_2/\text{a-MoS}_x$ sample can be expressed as $\text{TiO}_2/\text{a-MoS}_x\text{-Xp}$, where X represents the mass ratio of the Mo element to TiO_2 .

The structure of TiO_2 and amorphous MoS_x can be characterized by the XRD patterns (Fig. 7). The XRD results showed the characteristic peaks of MoS_x and TiO_2 , indicating that the amorphous MoS_x and TiO_2 successfully formed a composite.

To prove that the amorphous MoS_x phase has been successfully supported on the surface of the TiO_2 material, we analyzed the surface morphology and microstructure of the prepared $\text{TiO}_2/\text{a-MoS}_x$ photocatalyst by SEM, HRTEM and Mapping (Fig. 8). It was determined from the SEM and TEM pictures that MoS_x was successfully loaded onto the TiO_2 surface, and good contact was formed.

To prove the potential photocatalytic ability of the samples, we studied the hydrogen production capacity of the TiO_2 , a-MoS_x , $\text{TiO}_2+\text{a-MoS}_x$ mixed samples, $\text{TiO}_2/\text{c-MoS}_x$ and $\text{TiO}_2/\text{a-MoS}_x\text{-8p}$ samples. In Figure 9, the pure TiO_2 photocatalyst has almost no photocatalytic activity. This is due to the high photo-generated carrier recombination ability of TiO_2 , which limits its photocatalytic performance. The performance of the $\text{TiO}_2+\text{a-MoS}_x$ mixed sample was slightly higher than that of the pure TiO_2 sample, indicating that MoS_x and TiO_2 can form a certain charge transfer and improve the hydrogen evolution ability. After the surface of the TiO_2 photocatalyst material is modified with the a-MoS_x electronic promoter, the hydrogen evolution performance of the $\text{TiO}_2/\text{a-MoS}_x$ sample was greatly improved. Compared to the sample that simply mixes a-MoS_x and TiO_2 , the hydrogen evolution performance of the $\text{TiO}_2/\text{a-MoS}_x\text{-8p}$ sample is higher. This result shows that the direct loading of amorphous molybdenum sulfide on the surface of TiO_2 forms a better interface



Scheme 5 Schematic illustration showing the synthesis route of the $\text{TiO}_2/\text{a-MoS}_x$ nanoparticles.

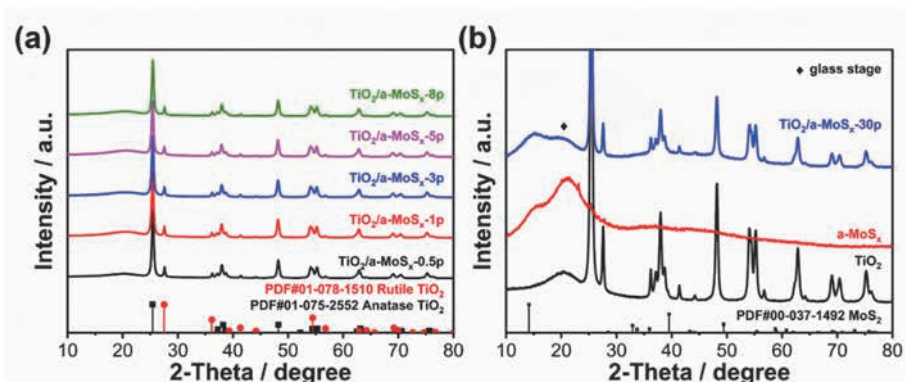


Fig. 7 (a,b) XRD results of the as-prepared samples

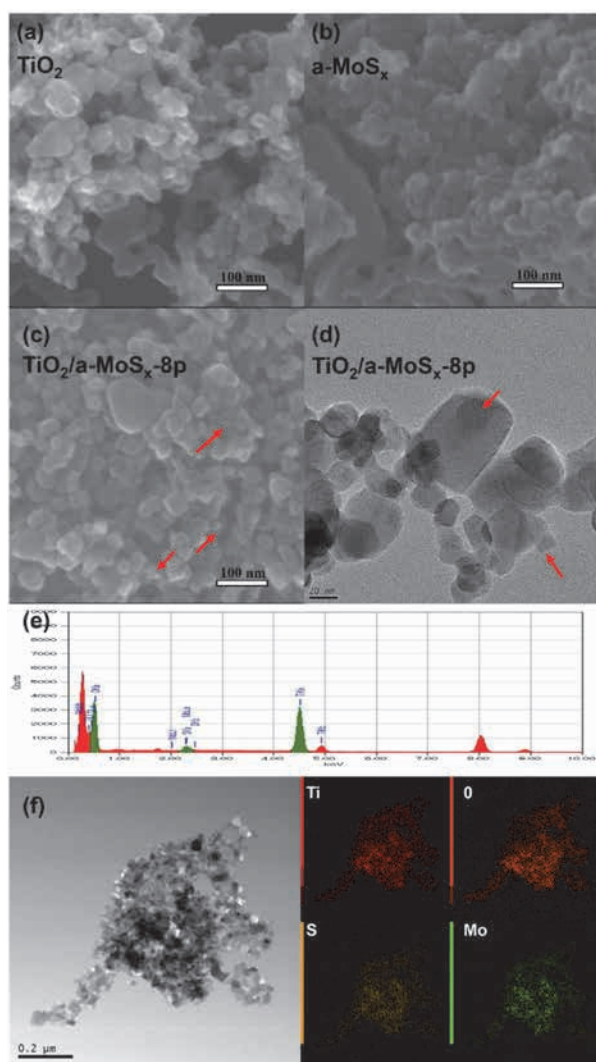


Fig. 8 SEM images of various samples: (a), (b), (c), (d), (e) EDS spectra of the $\text{TiO}_2/\text{a-MoS}_x$ -8p (f) HRTEM images and EDS elemental mapping images of the $\text{TiO}_2/\text{a-MoS}_x$ -8p

contact and has a faster electron transfer rate than simple mixing, thus improving the efficiency of the photocatalytic hydrogen evolution. Compared to the loaded crystalline molybdenum sulfide sample ($\text{TiO}_2/\text{c-MoS}_x$), the $\text{TiO}_2/\text{a-MoS}_x$ sample has a better hydrogen evolution performance. This is due to the abundant unsaturated S atoms on the surface of the amorphous molybdenum sulfide sample, which has more active sites. On the other hand, well-crystallized molybdenum sulfide catalysts usually need to be annealed (about 400°C), which can easily cause phase transitions between the anatase TiO_2 and amorphous MoS_2 , less unsaturated S atoms^[15] and a reduced specific surface area^[16], thus reducing the hydrogen evolution capacity of the catalyst.

A possible mechanism was proposed to explain the reason for the increase in the efficiency of the $\text{TiO}_2/\text{a-MoS}_x$ hydrogen production (Scheme 6). When a-MoS_x is loaded on the surface of TiO_2 , the $\text{TiO}_2/\text{a-MoS}_x$ hybrid forms a typical metal-semiconductor system. The work function of TiO_2 (4.2eV) is lower than that of a-MoS_x (5.7eV), which can force free electrons to migrate from TiO_2 to the amorphous MoS_x until the Fermi level is equal. For the amorphous MoS_x , it is obvious that due to its various lattice defects and irregular arrangements, there are more unsaturated S atoms inside and on the surface. These unsaturated S atoms can rapidly capture the hydrogen protons (H^+) in the solution, then obtain photoelectrons and reduce H^+ to H_2 . During the UV irradiation, the photoexcited electrons in the CB of TiO_2

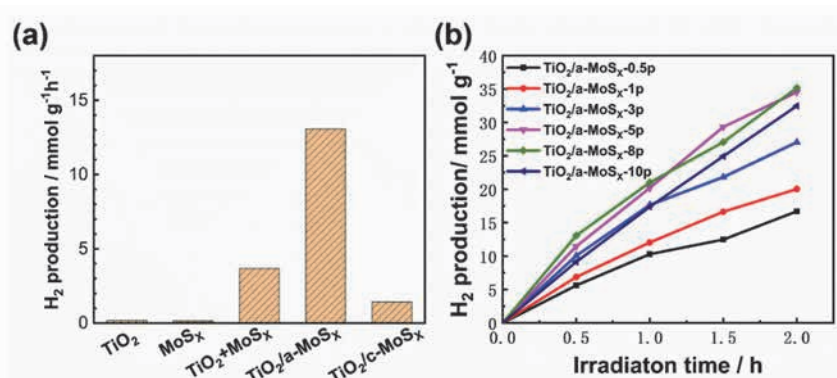
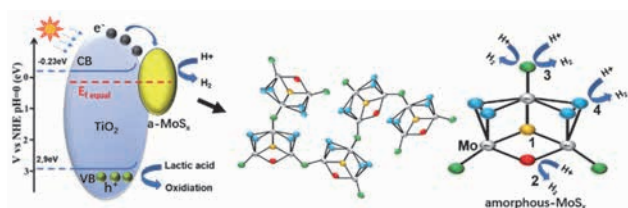


Fig. 9 Photocatalytic activity tests for H₂ evolution by the as-prepared samples under UV light.



Scheme 6 Schematic diagrams illustrating the possible photocatalytic mechanism of the TiO₂/a-MoS_x photocatalyst.

can be effectively transferred to the amorphous MoS_x, thereby promoting the interface charge transfer and subsequent hydrogen evolution reaction.

Due to the low impedance between the TiO₂ and a-MoS_x and the high-quality metal-semiconductor system, the constructed TiO₂/a-MoS_x hybrid can effectively separate photo-generated electrons and holes and move them to the surface of the a-MoS_x and TiO₂ particles, respectively. This is the reason for the highly-enhanced photocatalytic hydrogen production activity. Because of its high activity, easy preparation, low cost and high stability, the in-situ growth of a-MoS_x on the semiconductor photocatalyst by the adsorption-photodeposition conversion method is a very promising way for the preparation of efficient HER catalysts.

5. Conclusion

In this study, we used commercial TiO₂ as the main material and aimed to simplify the synthesis method and reduce the experimental cost. Cu, MoS_x and MoP are used to construct a catalytic system to improve the photocatalytic hydrogen production ability of the material. Good loading methods, such as in-situ deposition, ultrasonic adsorption, etc., were used to optimize the synthesis steps by promoting the transfer of electrons and holes between different materials and improving the photocatalytic performance of the composite materials. The photocatalytic reaction

mechanism was revealed by studying the morphology of the catalyst, the combination mode, the separation efficiency of the photogenerated carriers, and the photocatalytic hydrogen production activity under ultraviolet light. The result of this study provides technical support and a theoretical basis for the design and preparation of low-cost, simple and efficient photocatalytic systems.

References

- [1] G. Li, J. Huang, J. Chen, Z. Deng, Q. Huang, Z. Liu, W. Guo, R. Cao, Highly Active Photocatalyst of Cu₂O/TiO₂ Octahedron for Hydrogen Generation, *ACS Omega*, 4 (2019) 3392-3397.
- [2] W. Niu, T. Moehl, W. Cui, R. Wick-Joliat, L. Zhu, S.D. Tilley, Extended Light Harvesting with Dual Cu₂O-Based Photocathodes for High Efficiency Water Splitting, *Advanced Energy Materials*, 8 (2018).
- [3] M. Alegría, J. Aliaga, L. Ballesteros, C. Sotomayor-Torres, G. González, E. Benavente, Layered Nanocomposite 2D-TiO₂ with Cu₂O Nanoparticles as an Efficient Photocatalyst for 4-Chlorophenol Degradation and Hydrogen Evolution, *Topics in Catalysis*, 64 (2020) 167-180.
- [4] Z. Pu, I.S. Amiin, C. Zhang, M. Wang, Z. Kou, S. Mu, Phytic acid-derivative transition metal phosphides encapsulated in N,P-codoped carbon: an efficient and durable hydrogen evolution electrocatalyst in a wide pH range, *Nanoscale*, 9 (2017) 3555-3560.
- [5] Z. Pu, I.S. Amiin, X. Liu, M. Wang, S. Mu, Ultrastable nitrogen-doped carbon encapsulating molybdenum phosphide nanoparticles as highly efficient electrocatalyst for hydrogen generation, *Nanoscale*, 8 (2016) 17256-17261.
- [6] H. He, J. Lin, W. Fu, X. Wang, H. Wang, Q. Zeng, Q. Gu, Y. Li, C. Yan, B.K. Tay, C. Xue, X. Hu, S.T. Pantelides, W. Zhou, Z. Liu, MoS₂/TiO₂ Edge-On Heterostructure for Efficient Photocatalytic Hydrogen Evolution, *Advanced*

- Energy Materials, 6 (2016).
- [7] X. Liu, Z. Xing, H. Zhang, W. Wang, Y. Zhang, Z. Li, X. Wu, X. Yu, W. Zhou, Fabrication of 3 D Mesoporous Black TiO_2 / MoS_2 / TiO_2 Nanosheets for Visible-Light-Driven Photocatalysis, *ChemSusChem*, 9 (2016) 1118-1124.
- [8] H. Wang, X. Xiao, S. Liu, C.L. Chiang, X. Kuai, C.K. Peng, Y.C. Lin, X. Meng, J. Zhao, J. Choi, Y.G. Lin, J.M. Lee, L. Gao, Structural and Electronic Optimization of MoS_2 Edges for Hydrogen Evolution, *J Am Chem Soc*, 141 (2019) 18578-18584.
- [9] L. Yi, F. Lan, J. Li, C. Zhao, Efficient Noble-Metal-Free Co-NG/ TiO_2 Photocatalyst for H_2 Evolution: Synergistic Effect between Single-Atom Co and N-Doped Graphene for Enhanced Photocatalytic Activity, *ACS Sustainable Chemistry & Engineering*, 6 (2018) 12766-12775.
- [10] B.H. Lee, S. Park, M. Kim, A.K. Sinha, S.C. Lee, E. Jung, W.J. Chang, K.S. Lee, J.H. Kim, S.P. Cho, H. Kim, K.T. Nam, T. Hyeon, Reversible and cooperative photoactivation of single-atom Cu/ TiO_2 photocatalysts, *Nat Mater*, 18 (2019) 620-626.
- [11] H. Hamad, E. Bailón-García, F.J. Maldonado-Hódar, A.F. Pérez-Cadenas, F. Carrasco-Marín, S. Morales-Torres, Synthesis of TixOy nanocrystals in mild synthesis conditions for the degradation of pollutants under solar light, *Applied Catalysis B: Environmental*, 241 (2019) 385-392.
- [12] D. Ariyanti, L. Mills, J. Dong, Y. Yao, W. Gao, NaBH_4 modified TiO_2 : Defect site enhancement related to its photocatalytic activity, *Materials Chemistry and Physics*, 199 (2017) 571-576.
- [13] D. Kato, K. Hongo, R. Maezono, M. Higashi, H. Kunioku, M. Yabuuchi, H. Suzuki, H. Okajima, C. Zhong, K. Nakano, R. Abe, H. Kageyama, Valence Band Engineering of Layered Bismuth Oxyhalides toward Stable Visible-Light Water Splitting: Madelung Site Potential Analysis, *J Am Chem Soc*, 139 (2017) 18725-18731.
- [14] L. Zhang, Y. Yang, M.A. Ziaee, K. Lu, R. Wang, Nanohybrid of Carbon Quantum Dots/Molybdenum Phosphide Nanoparticle for Efficient Electrochemical Hydrogen Evolution in Alkaline Medium, *ACS Appl Mater Interfaces*, 10 (2018) 9460-9467.
- [15] H. Yu, R. Yuan, D. Gao, Y. Xu, J. Yu, Ethyl acetate-induced formation of amorphous MoS_x nanoclusters for improved H_2 -evolution activity of TiO_2 photocatalyst, *Chemical Engineering Journal*, 375 (2019).
- [16] Y. Yu, J. Wan, Z. Yang, Z. Hu, Preparation of the MoS_2 / TiO_2 /HMFs ternary composite hollow microfibres with enhanced photocatalytic performance under visible light, *J Colloid Interface Sci*, 502 (2017) 100-111.